Chemical Engineering Journal 155 (2009) 83–87

Contents lists available at ScienceDirect

Chemical Engineering Journal

journal homepage: www.elsevier.com/locate/cej

Yttrium-doped TiO_2 films prepared by means of DC reactive magnetron sputtering

Wenjie Zhang[a,b,*], Kuanling Wang[a], Shenglong Zhu[b], Ying Li[b], Fuhui Wang[b], Hongbo He[c]

[a] School of Environmental and Chemical Engineering, Shenyang Ligong University, Shenyang Hun-Nan, Shenyang 110168, China
[b] State Key Laboratory for Corrosion and Protection, Institute of Metal Research, The Chinese Academy of Sciences, Shenyang 110016, China
[c] Institute of Applied Ecology, The Chinese Academy of Sciences, Shenyang 110016, China

ARTICLE INFO

Article history:
Received 10 April 2009
Received in revised form 17 June 2009
Accepted 24 June 2009

Keywords:
TiO_2 film
Reactive magnetron sputtering
Yttrium doping
Photocatalytic activity
Degradation

ABSTRACT

Y_2O_3-doped TiO_2 films were prepared on glass substrates by means of pulsed DC reactive magnetron sputtering method using titanium and yttrium mixed target. XPS results showed that the films were composed of fully oxidation states of the two elements, Y_2O_3–TiO_2 composite oxides. The existence of yttrium inhibited the crystal growth of TiO_2 in the films and Y_2O_3 mainly presented in its amorphous state in the films. UV–vis transmittance of the films decreased whereas their reflectance increased slightly. Yttrium doping had detrimental effect on photocatalytic activity of the TiO_2 films. Photocatalytic degradation efficiency of methyl orange solution declined along with increasing yttrium concentration.

1. Introduction

TiO_2 has showed many good aspects such as high activity, low cost and stable and has been applied to a variety of environmental problems as a main photocatalyst especially in water and air purification. Besides the originated discovery of photo-splitting of water under UV and solar irradiations, its application has been extended to various environmental pollution treatments. As a very popular research area, surface modification methods such as noble metal doping [1,2], composite semiconductors and transition metal doping [3–5] have aroused much attention in improving photocatalytic activity of TiO_2.

Although nano-sized TiO_2 particles with large surface area have high photocatalytic activity, it is hard to separate small particles from the slurry after water treatment. TiO_2 film has gradually become a research focus in this field. Several kinds of deposition methods can be used to immobilize TiO_2 films onto different kinds of supporters [6–8]. Magnetron sputtering is an interesting method for preparing TiO_2 film because it is an industrial process applicable to large-area deposition, and high quality TiO_2 films can be achieved even at low substrate temperatures [9,10].

Rare earth metal doping is an effective method to enhance photocatalytic activity [11–13]. It is reported that the optimal doping concentration is around 0.5%. At the same time, some kinds of rare earth metals have no contribution in improving photocatalytic activity [14].

In our previous studies, we have prepared metal-doped TiO_2 films through reactive magnetron sputtering using mixed titanium and doping metal target, instead of alloy target. Fe- and Cu-doped TiO_2 films have been prepared by using this method [15,16]. In this paper, yttrium-doped TiO_2 films were prepared on glass substrates by means of DC reactive magnetron sputtering method using Y–Ti mixed target. Structural and photocatalytic properties of the films were investigated.

2. Experimental

2.1. Preparation of TiO_2 film

The TiO_2 thin films were deposited on microscope glass slides (75 mm × 25 mm × 1.5 mm) by means of DC magnetron sputtering system (SBH-5115D). The DC power supplies were Advanced Energy Pinnacle 6 kW and MDX Sparc-LE 20 that were set at the active arc-handling mode.

The target was titanium with a purity of 99.9% and surface area of 125 mm × 378 mm. Thin yttrium pieces with purity of 99.9% were fixed on the titanium target using screws made of pure titanium. The substrates of microscope glass slides were fixed on the anode that was made of 2 mm thick steel plate. Substrate temperature was

* Corresponding author at: School of Environmental and Chemical Engineering, Shenyang Ligong University, Shenyang Hun-Nan, Shenyang 110168, China. Tel.: +86 24 83978969.
E-mail address: metalzhang@yahoo.com.cn (W. Zhang).

1385-8947/$ – see front matter © 2009 Elsevier B.V. All rights reserved.
doi:10.1016/j.cej.2009.06.039

determined using a thermocouple detector on the steel plate. The distance between target and substrate was 150 mm. After the chamber was evacuated to a vacuum lower than 1.2×10^{-3} Pa, argon was introduced into the chamber and discharge began at a constant current of 2.5 A. After the discharge colour changed from pink to blue and the discharge voltage maintained at a low value, oxygen was introduced into the chamber. The argon and oxygen flow rates were 14.15 and 7.45 ml/min, respectively. All of the films were deposited for 5 h and the substrate temperature was below 130 °C. An average film thickness of 160 nm per hour was achieved at a constant discharge current of 2.5 A.

2.2. Film characterization

The crystalline structure was measured using X-ray diffraction (XRD) with a Cu Kα source and the grain size was calculated using Scherrer's formula. The yttrium concentration was measured by electron probe microanalysis (EPMA). The surface morphology of the film was observed by scanning electron microscope (SEM). The samples for SEM imaging were coated with a thin layer of gold film to avoid charging. The film composition and titanium oxidation state were determined using X-ray photoelectron spectroscopy (XPS). The optical transmission and reflectance spectra of the films were measured at room temperature in air using a Shimadzu UV-265 spectrophotometer and a DMR-22 spectrophotometer, respectively. The thickness of the films was calculated using Swanepoel's method [17] through UV–vis transmission spectra.

The photocatalytic activity of the TiO_2 films was evaluated by measuring the degradation rate of aqueous methyl orange on the films under UV irradiation. In each experiment, a TiO_2 film of 25 mm × 25 mm was settled on the bottom of a 100 ml beaker, which contained 30 ml aqueous methyl orange. The beaker was immersed into a thermostatic bath at 30 °C. A 125 W high-pressure mercury lamp was suspended 13.5 cm above the TiO_2 films. The average intensity of UV irradiation was 4.5 mW/cm^2 by measuring with a UV irradiation meter (Model UV-A), whose wavelength range and peak wavelength were 320–400 and 365 nm, respectively. Air was pumped into the solution at the flow rate of 100 ml/min in order to supply oxygen for the degradation and stir the solution. Methyl orange concentration during irradiation was measured by Shimadzu UV-265 spectrophotometer, and the initial concentration was 20 mg/l.

3. Results and discussion

3.1. Film preparation

The mixed target used in this paper has its special advantage. The concentration of yttrium doped into the TiO_2 films can be controlled simply by adjusting the size of yttrium pieces fixed on the titanium target. However, an alloy target made from titanium and yttrium has a fixed Ti/Y ratio and can only be used to prepare yttrium-doped TiO_2 with a specified yttrium concentration.

In order to prepare a series of TiO_2 samples containing different percentage of yttrium, pure yttrium pieces were fixed on the titanium target and sputtered in mixed argon and oxygen gases. After oxygen flow rate reached the threshold, the target was covered with titanium oxides and yttrium oxides. In order to prepare Y-doped TiO_2 film, titanium oxides and yttrium oxides should be sputtered onto the substrate simultaneously during magnetron sputtering process.

Table 1 shows yttrium concentration in the TiO_2 films deposited for 5 h under discharge current of 2.5 A. All the doped films exhibited similar physical appearance as compared to pure TiO_2 film which is transparent and colorless.

Table 1
Yttrium concentration in the TiO_2 films.

Sample	D	E	F	G	H	I	J	K
Y piece area/mm^2	1295	720	360	260	120	60	45	30
Y/(Y + Ti)/at.%	11.28	10.02	6.79	3.23	1.74	1.51	0.71	0.38

As shown in Fig. 1, while working at constant argon flow rate and discharge current, the discharge voltage increased when oxygen flow rate increased from zero up to the threshold, indicating the narrowing of the metal area being sputtered. When oxygen flow rate reached the threshold, an abrupt increase of discharge voltage occurred, due to full coverage of oxide on the target. After that, the target voltage decreased to a stable value in the compound sputtering mode. This can be explained by an increase of the secondary electron emission yield because of coverage of the target by oxides [18]. The threshold of oxygen flow rate remained constant when yttrium piece area increased from 30 to 1295 mm^2. However, discharge voltage had apparent difference with different yttrium piece area.

Oxygen partial pressure is a function that may influence the discharge parameters such as plasma potential, discharge voltage, deposition rate, and ion composition of the discharge. A mixture of metallic Ti and titanium oxides is deposited on the substrate before the threshold. Only after the oxygen flow rate reaches the threshold, a uniform transparent TiO_2 thin film can form on the substrate. For this reason, the TiO_2 films were prepared at an oxygen flow rate 0.7 ml/min higher than its threshold in this paper.

3.2. Film characterization

Fig. 2 shows the XPS survey spectra for the surface of the deposited pure and Y-doped TiO_2 films. The deposited pure TiO_2 film contains Ti and O elements, and the Y-doped TiO_2 films also contain yttrium element. The C 1s peak is due to the adsorbed carbon. The photoelectron peak for Ti 2p can be seen at a binding energy (E_b) of 458 eV, so does O 1s at E_b = 530.3 eV, C 1s at E_b = 284 eV, and Y 3d at E_b = 158.3 eV.

Fig. 3 shows the XPS spectra of Ti 2p, Y 2p and O 1s regions for the surface of the deposited TiO_2 film. A main doublet composed of two symmetric peaks situates at E_b (Ti $2p_{3/2}$) = 458.4 eV and E_b (Ti $2p_{1/2}$) = 464.2 eV is assigned to Ti^{4+} [19]. The doped yttrium has minor influence on titanium oxidation state of the deposited film.

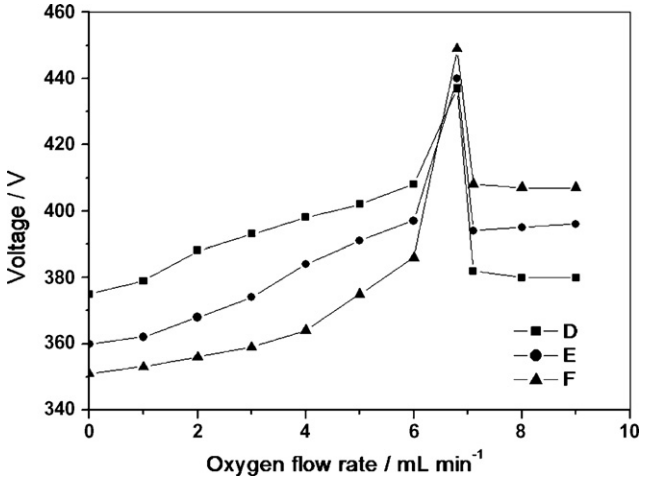

Fig. 1. Discharge voltage at different oxygen flow rates during reactive magnetron sputtering.

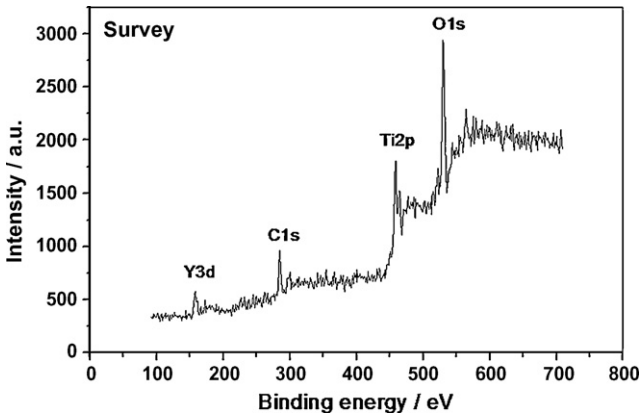

Fig. 2. XPS survey spectrum of the Y-doped TiO_2 film.

The binding energies of Ti 2p region for Y-doped samples are almost the same as compared to that of pure TiO_2 films. Only Ti^{4+} was found in the pure and Y-doped TiO_2 film deposited in the compound mode after oxygen flow rate surpasses the threshold. Y_2O_3 is characterized by the peak at the binding energy of 158.3 eV in the XPS spectra of Y 3d for the surface of Y-doped TiO_2 films [20,21]. Oxygen is in the form of O^{2-} in the deposited films that can be seen from its XPS spectrum [22]. As for the circumstances in the chamber as well as the low deposition temperature, the yttrium oxide deposited on the substrate in the combined conditions was in the fully oxidized state of Y_2O_3. Metal Y was not found in the deposited Y-doped TiO_2 films.

The XRD patterns of the yttrium-doped and pure TiO_2 films are shown in Fig. 4. Sample J with yttrium concentration of 0.71 at.% was in the anatase phase. This is in accordance with pure TiO_2 film deposited under the same conditions. Further increase of yttrium concentration inhibited the crystal growth in the TiO_2 films and the samples became amorphous while there was no crystalline Y_2O_3 formed in the deposited film either. Crystalline titanium oxide could not grow in the highly yttrium-doped films.

SEM images for the surface of the Y-doped and pure TiO_2 films are shown in Fig. 5. The surface morphology gradually changed from rough to flat along with the increase of doped yttrium concentration. When the amount of doped yttrium was lower than 1.5 at.%, the surface morphology was similar to that of pure TiO_2 film. As shown in the SEM image of sample K, the film was composed of nano-particles of TiO_2 with nano-sized holes, which could provide more surface area for photocatalytic process than flat film or films composed of large particles. These particles were mainly composed of titanium oxide and a small amount of yttrium oxide was well distributed in the particles. The formation of anatase TiO_2 crystals has increased the surface roughness and thus resulted in the holes morphology on the surface.

UV–vis transmittance and reflectance spectra of samples D and I are shown in Figs. 6 and 7. When yttrium dopant concentration in the films increased from 1.51 to 11.28 at.%, UV–vis transmittance went down slightly, whereas, the reflected light increased about 3%. The increase of reflectance is mainly due to the retarded formation of titanium oxide in the films containing high concentration of yttrium. The resulted flat surface of the films could reflect more irradiation and lead to lower transmission. Yttrium in the films cannot make any influence on light absorbance of the films because yttrium oxide has no response in the visible region of light spectra and cannot make any contribution to film absorption behavior.

Absorption edge of yttrium-doped TiO_2 films exhibited blue shift, as shown in Fig. 6. The absorption edge of sample D slightly moves to shorter wavelength region compared with sample I.

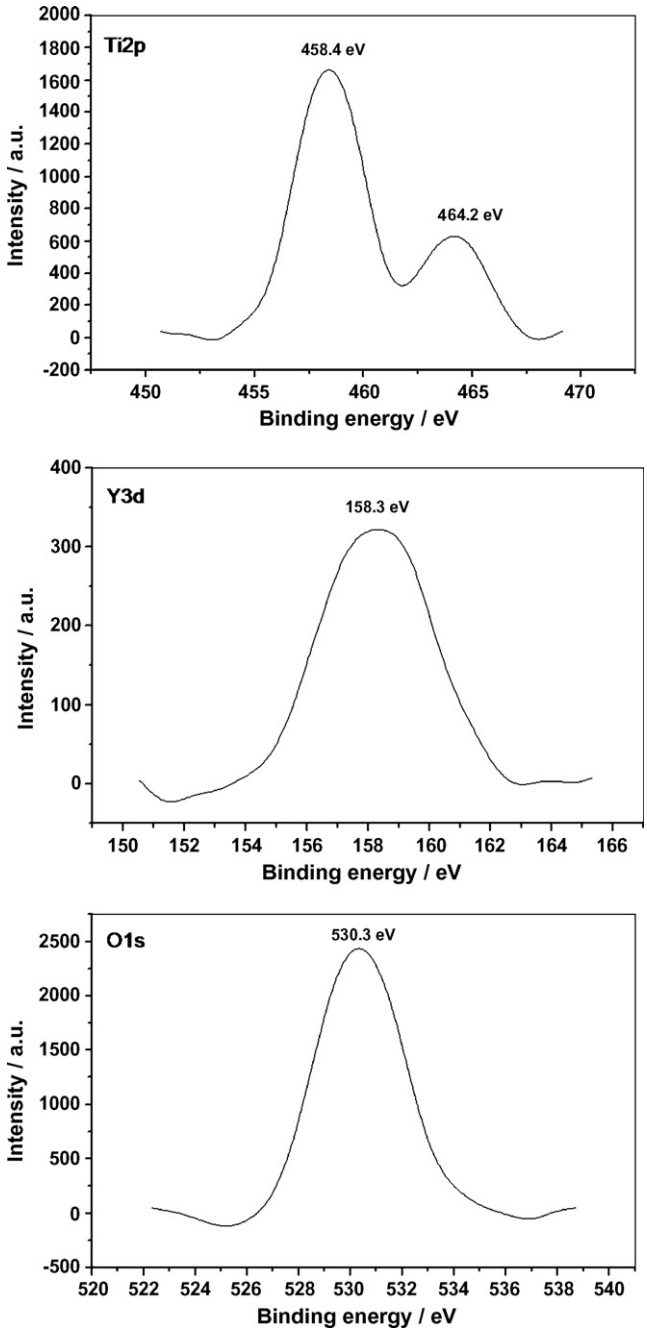

Fig. 3. XPS spectra of the elements in the Y-doped TiO_2 film.

That means photons with higher energy are needed to initiate electron–hole generation. Thus, the response region of the films containing high Y_2O_3 concentration shrinks further to shorter wavelength region.

3.3. Photocatalytic activity

Fig. 8 shows methyl orange degradation rates during 180 min irradiation on the yttrium-doped and pure TiO_2 films. As can be seen from the figure, methyl orange degradation rate declined constantly with increasing concentration of doped yttrium. Yttrium doping exhibited a detrimental effect on photocatalytic activities of the films. When yttrium concentration exceeded 2 at.%, the photocatalytic activity of the films decreased apparently. After yttrium concentration was more than 10 at.%, the films nearly lost their photocatalytic activities.

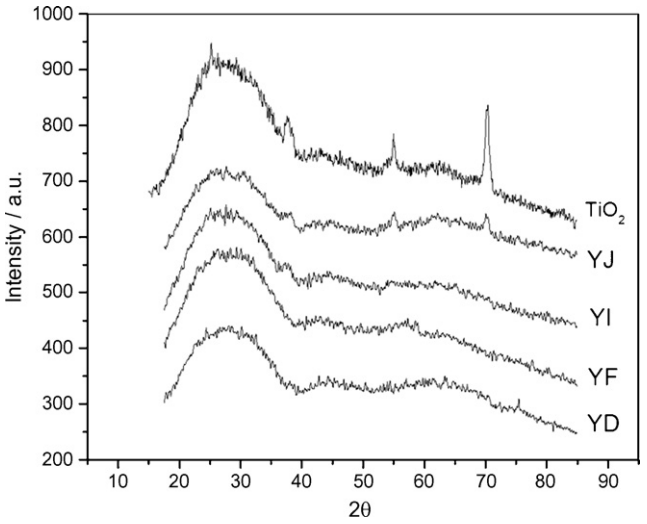

Fig. 4. XRD patterns of the Y-doped and pure TiO_2 films.

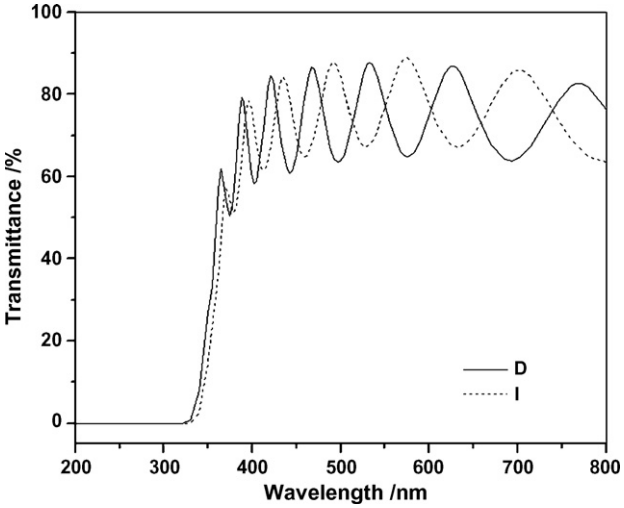

Fig. 6. UV–vis transmittance spectra of the Y-doped TiO_2 films.

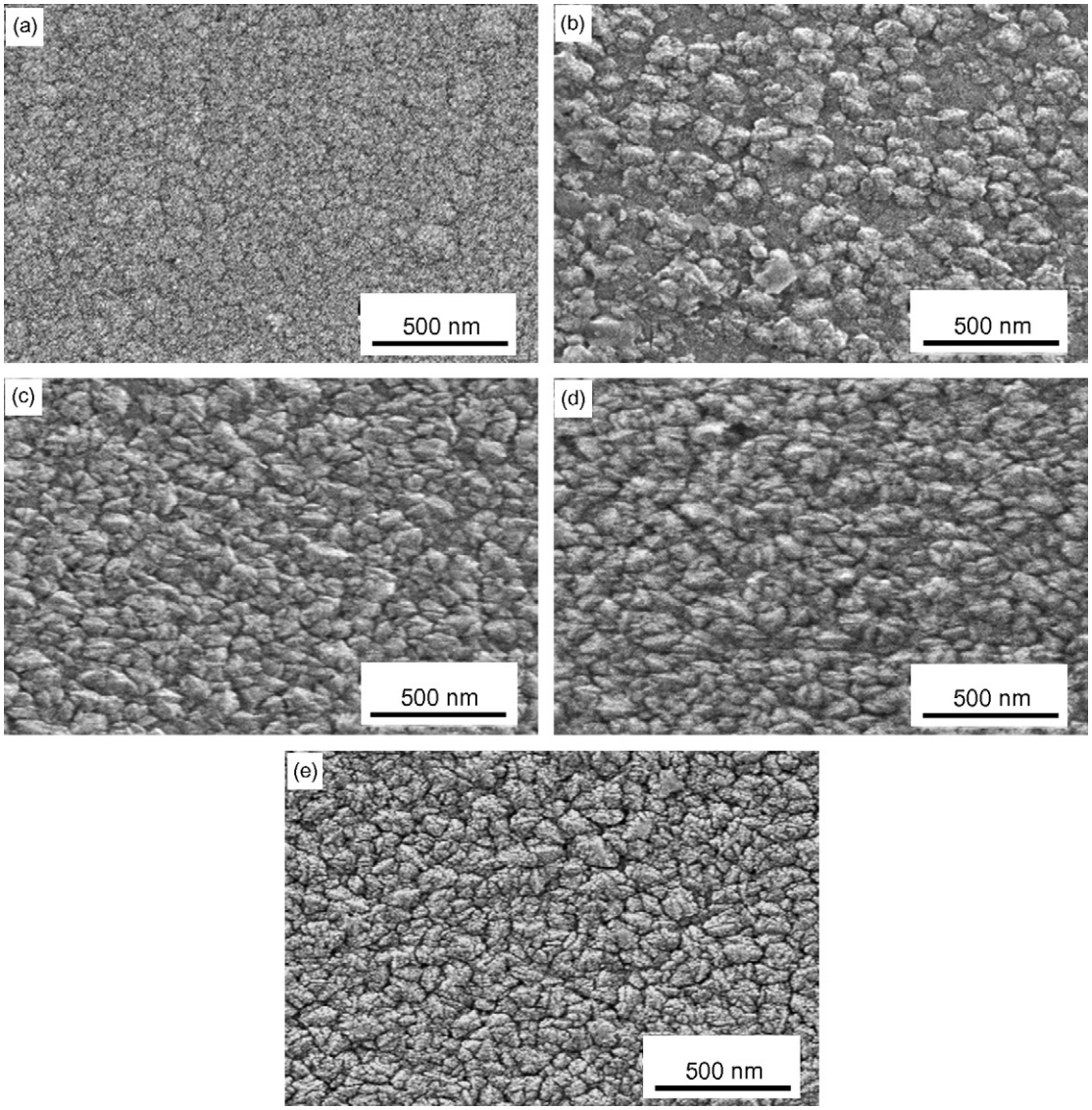

Fig. 5. SEM images of the Y-doped and pure TiO_2 films: (a) F, (b) I, (c) J, (d) K and (e) pure TiO_2.

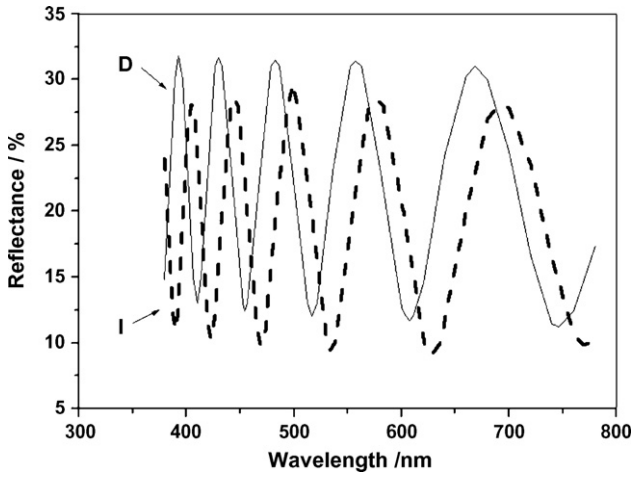

Fig. 7. UV–vis reflectance spectra of the Y-doped TiO_2 films.

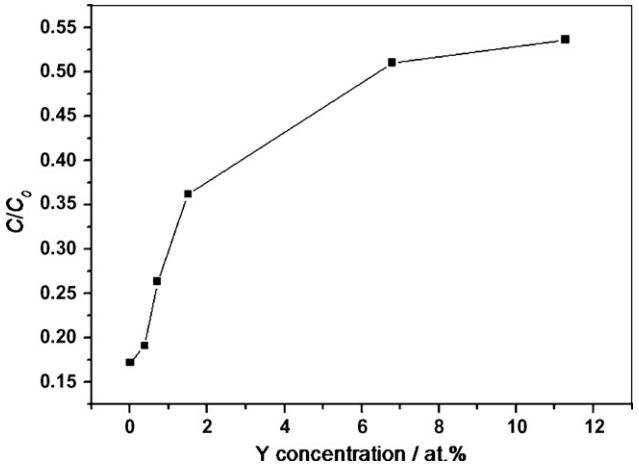

Fig. 8. Photocatalytic degradation of methyl orange on the Y-doped TiO_2 films. (C_0 is initial aqueous methyl orange concentration of 20 mg l^{-1} and C is aqueous methyl orange concentration after 180 min irradiation.)

The decrease of photocatalytic activities of yttrium-doped TiO_2 films was due to two reasons. Firstly, yttrium doping could not improve light absorption behavior of the TiO_2 films. Secondly, the existence of yttrium in the films inhibited TiO_2 crystal formation, and resulted in lower crystallinity and weaker photocatalytic activity of the films, because TiO_2 films with small particle size has better photocatalytic activity than the films containing large particles or in the amorphous form.

4. Conclusions

Yttrium-doped TiO_2 films were prepared by means of DC reactive magnetron sputtering using mixed Y–Ti target. Yttrium pieces were fixed on the pure titanium target so that yttrium concentration in the deposited films could be controlled by simply changing yttrium pieces area. The deposited films are composed of TiO_2 and Y_2O_3. Yttrium doping has detrimental effect on TiO_2 crystalline formation, and the intensity of TiO_2 XRD peaks decreases with increasing yttrium concentration. Y_2O_3 is in its amorphous phase in the doped TiO_2 films.

The doped yttrium cannot enhance light absorption capacities of the TiO_2 films. On the contrary, photocatalytic methyl orange degradation rate declines with increasing yttrium concentration.

Acknowledgment

This work was supported by the National Natural Science Foundation of China (No. 50774074).

References

[1] M. Hoffmann, S.T. Martin, W. Choi, W. Bahnemann, Environmental applications of semiconductor photocatalysis, Chem. Rev. 95 (1995) 69–96.
[2] O. Legrini, E. Oliveros, A.M. Braun, Photochemical processes for water treatment, Chem. Rev. 93 (1993) 671–698.
[3] M.A. Barakat, H. Schaeffer, G. Hayes, S. Ismat-Shah, Photocatalytic degradation of 2-chlorophenol by co-doped TiO_2 nanoparticles, Appl. Catal. B 57 (2005) 23–30.
[4] X.H. Wang, J.G. Li, H. Kamiyama, Y. Moriyoshi, T. Ishigaki, Wavelength-sensitive photocatalytic degradation of methyl orange in aquenos suspension over iron(III)-doped TiO_2 nanopowders under UV and visible light irradiation, J. Phys. Chem. B 110 (2006) 6804–6809.
[5] S. Rengaraj, X.Z. Li, P.A. Tanner, Z.F. Pan, G. Pang, Photocatalytic degradation of methylparathion—an endocrine disruptor by Bi^{3+}-doped TiO_2, J. Mol. Catal. A 247 (2006) 36–43.
[6] T.A. McMurray, P. Dunlop, J.A. Byrne, The photocatalytic degradation of atrazine on nanoparticulate TiO_2 films, J. Photochem. Photobiol. A 182 (2006) 43–51.
[7] Z.S. Guan, X.T. Zhang, Y. Ma, Y.A. Cao, J.N. Yao, Photocatalytic activity of TiO_2 prepared at low temperature by a photoassisted sol–gel method, J. Mater. Res. 16 (2001) 907–909.
[8] H. Yahiro, T. Miyamoto, N. Watanabe, H. Yamaura, Photocatalytic partial oxidation of a-methylstyrene over TiO_2 supported on zeolites, Catal. Today 120 (2007) 158–162.
[9] W.J. Zhang, Y. Li, F.H. Wang, Properties of TiO_2 thin films prepared by magnetron sputtering, J. Mater. Sci. Technol. 18 (2002) 101–107.
[10] P. Lobl, M. Huppertz, D. Mergel, Nucleation and growth in TiO_2 films prepared by sputtering and evaporation, Thin Solid Films 251 (1994) 72–79.
[11] A.W. Xu, Y. Gao, H.Q. Liu, The preparation, characterization, and their photocatalytic activities of rare-earth-doped TiO_2 nanoparticles, J. Catal. 207 (2002) 151–157.
[12] Y.B. Xie, P. Li, C.W. Yuan, Visible-light excitated photocatalytic activity of rare earth metal–ion-doped titania, J. Rare Earth 20 (2002) 619–625.
[13] K.M. Parida, N. Sahu, Visible light induced photocatalytic activity of rare earth titania nanocomposites, J. Mol. Catal. A 287 (2008) 151–158.
[14] J. Lin, J.C. Yu, An investigation on photocatalytic activities of mixed TiO_2–rare earth oxides for the oxidation of acetone in air, J. Photochem. Photobiol. A 116 (1998) 63–67.
[15] W.J. Zhang, Y. Li, S.L. Zhu, F.H. Wang, Copper doping in titanium oxide catalyst film prepared by dc reactive magnetron sputtering, Catal. Today 93–95 (2004) 589–594.
[16] W.J. Zhang, Y. Li, S.L. Zhu, F.H. Wang, Surface modification of TiO_2 film by iron doping using reactive magnetron sputtering, Chem. Phys. Lett. 373 (2003) 333–337.
[17] R. Swanepoel, Determination of the thickness and optical constants of amorphous silicon, J. Phys. E 16 (1983) 1214–1222.
[18] R. Gouttebaron, D. Cornelissen, R. Snyders, J.P. Dauchot, M. Wautelet, M. Hecq, XPS study of TiO_x films prepared by d.c. magnetron sputtering in Ar–O_2 gas mixtures, Surf. Interface Anal. 30 (2000) 527–530.
[19] J. Pouilleau, D. Devilliers, H. Groult, P. Marcus, Surface study of a titanium-based ceramic electrode material by X-ray photoelectron spectroscopy, J. Mater. Sci. 32 (1997) 5645–5651.
[20] J.M. Gao, H.N. Xiao, H. Du, Effect of Y_2O_3 addition on ammono sol–gel synthesis and sintering of Si_3N_4–SiC nanocomposite powder, Ceram. Int. 29 (2003) 655–661.
[21] Y. Baba, T.A. Sasaki, Application of X-ray-induced auger electron spectroscopy to state analyses of hydrogen implanted in Y, Zr and Nb metals, Surf. Interface Anal. 6 (1984) 171–173.
[22] R.P. Netterfield, P.J. Martin, C.G. Pacey, W.G. Sainty, D.R. McKenzie, Ion-assisted deposition of mixed TiO_2–SiO_2 films, J. Appl. Phys. 66 (1989) 1805–1809.